1/*f* ruffle oscillations in plasma membranes of amphibian epithelial cells under normal and inverted gravitational orientations

H. S. Silva,[1] M. L. Martins,[2,*] M. J. Vilela,[3] Ruy Jaeger,[4] and B. Kachar[5]
[1]*Departamento de Física, Universidade Federal de Pernambuco, 50670-901 Recife PE, Brazil*
[2]*Departamento de Física, Universidade Federal de Viçosa, 36570-000 Viçosa, MG, Brazil*
[3]*Departamento de Biologia Animal, Universidade Federal de Viçosa, 36570-000 Viçosa, MG, Brazil*
[4]*Departamento de Biologia Celular e do Desenvolvimento, Instituto de Ciências Biomédicas, Universidade de São Paulo, 05508-900 São Paulo, SP, Brazil*
[5]*Laboratory of Cellular Biology,National Institutes on Deafness and other Communication Disorders, National Institutes of Health, 50 South Drive, Bethesda, Maryland 20892-8027, USA*

(Received 7 March 2006; revised manuscript received 20 July 2006; published 4 October 2006)

Membrane ruffle fluctuations of amphibian epithelial cells A6 (CCL102) cultured in normal and upside down oriented plates have been analyzed through video microscopy. Our results reveal that their edge ruffle fluctuations exhibit a stochastic dynamics with $1/f^{\alpha}$ power spectrum over at least two decades at low frequencies and long range correlated, self-affine lateral border profiles. In a few and small areas of the membrane, probably nearby focal contacts, we found periodic oscillations which could be induced by myosin driven contraction of stress fibers. Furthermore, whereas the different gravitational orientations had none or little effect on the structure (power spectra and surface roughness) of these membrane ruffle fluctuations, their dynamic parameters were differentially affected. Indeed, the decay time of ruffles remained unchanged, but the period of lamellipodia oscillations near the focal adhesion points was significantly altered in A6 cells cultured upside down.

DOI: 10.1103/PhysRevE.74.041903 PACS number(s): 87.16.Qp, 87.16.Dg, 87.15.Ya, 87.17.Jj

I. INTRODUCTION

Cell-sized movements play a major role in a large range of biological processes [1]. Migrating cells shape organs and tissues in developing embryos take part in immune response, angiogenesis, wound healing, and are involved in many diseases such as metastatic cancer, arthritis, and neurological birth defects. Cell movements in eukaryotes proceed through a complex cycle of extension, attachment, towing, and detachment. These cells extend protrusions, called lamellipodia, to push their membranes outward, attach them to the extracellular matrix by forming adhesion structures, move the bulk of their cell bodies using adhesions as point of traction, and finally release their rear attachments, ending the cycle of motion. So, several molecular motors, adhesion proteins (particularly integrins), and large dynamic rearrangements of cell cytoskeleton are involved in cell movement.

About thirty years after the work of Brochard and Lennon concerning the frequency spectrum of the flicker oscillations in red blood cells [2], there is a renewed interest in understanding the mechanical properties and migration dynamics of a wide variety of living cells [3]. Indeed, under normal circumstances, lipid bilayers and cell membranes are flexible and do not behave as random surfaces, but exhibit both equilibrium (e.g., thermally excited bending undulations) and nonequilibrium fluctuations (e.g., lamellipodium or filopodium protrusion and retraction) which lead to fluctuation-induced interactions. The spectrum of shape fluctuations contains a wide range of length scales from about 1 nm (displacement of single molecules) to about 10 μm (flicker modes of vesicles and cells) [5]. In 1991, Levin and Korenstein demonstrated that the dominant component of membrane fluctuations in erythrocytes are linked to a MgATP-dependent dynamic assembly of the cytoskeleton [6]. However, only recently the basic mechanism involved in such flicker phenomenon was elucidated by Gov and Safran [7]. Their theoretical work has shown that ATP-induced dynamic dissociations of spectrin filaments in the cytoskeleton network can explain both shape transformations and fluctuation amplitude in the membrane of red blood cells. In turn, experiments using artificial vesicles have provided relevant information about the properties of biological membranes. For instance, observations of the self-assembly of thin actin shells in giant vesicles demonstrate that shape changes, such as buckling and blister formation, generate a $1/f^{\alpha}$ noise (with $\alpha=1.3$) for the vesicle fluctuating contour [8]. Also, experiments with giant unilamellar vesicles containing the transmembrane protein Ca^{2+}-ATPase revealed that their pumping activities enhance membrane fluctuations, a nonequilibrium effect requiring ATP hydrolysis [4].

In contrast to the former phenomena, in eukaryotic cells, membrane dynamics is qualitatively new and more complex as it is illustrated by the sustained periodic oscillations in the height of 3T3 fibroblasts at a frequency of 4.9 Hz due to periodic contractions of stress fibers [9]. Actin-based cell motility involves the coupling of plasma membranes with cytoskeletal networks made of motor proteins (myosin) interacting with polar filaments (actin) which polymerize and depolymerase. From the physical point of view, it seems that the essential features underlying the mechanical functions of a liquidlike cell are ascribed to its cytoskeleton, a glassy material which some researchers claim to exist close to a glass transition [10]. Conjectures apart, the cytoskeleton is a

*Electronic address: mmartins@mail.ufv.br

viscoelastic gel driven away from equilibrium by ATP hydrolysis for both actin polymerize and depolymerize and myosin activation. Therefore this is an example of the so-called active gels which work at the expenses of permanent energy consumption [11]. In such active gels, behaviors which would be static in the absence of energy input or in a passive gel become dynamic. Relaxation modes which would be entirely damped in low frequencies can now generate traveling waves. Also, in active gels, topological defects (asters, spirals, and vortexes) can start and rotate permanently [12,13].

Concerning cell migration, the lamellipodium is an active gel enclosed in a flat membrane extension adhered to the substrate. The receding of lamellipodia protrusions generate significant increases in the curvature of the plasma membrane, caused by bursts of actin polymerization in the cytoskeleton, that move towards the cell nucleus. Similar ruffles, associated to macropinnocytosis and phagocytosis processes, are also formed over the cell membrane away from lamellipodia extension sites. Recently, Agero *et al.* applied defocusing microscopy [14], which provides a portrait of the curvature of the phase object, to study surface curvature fluctuations of macrophages even during phagocytosis process [15,16]. These authors were able to observe single phagocytosis events and identified two main types of membrane fluctuations: small random flickers that permeate the whole cell and large coherent (kinklike) structures that propagate from the edge towards the nucleus of the cell. Furthermore, they obtained a positive correlation between the amount of surface fluctuations of a single macrophage and phagocytosis time.

The present paper focuses active membrane fluctuations of amphibian epithelial cells A6 CCL102 observed by video microscopy, particularly in cells cultured upside down. Specifically, the evolution in time of edge ruffles related to lamellipodia dynamics is studied. These coherent structures bordering the cell [15,16] are those with strong enough thickness to be observed through the phase-contrast microscopy used here. The main goal is to investigate cell response to the gravitational stress, which is mediated by membrane proteins (mechanosensitive channels) attached to the cytoskeleton and designed to the sensing of physical forces.

The paper is organized as follows: in Sec. II, the details of cell culture, video microscopy, mapping of cell borders in radial profiles, and the quantitative methods used to analyze such profiles are presented; in Sec. III, the obtained results are reported and discussed in Sec. IV; finally, in Sec. V some conclusions are drawn.

II. METHODS

A. Cell culture

Amphibian epithelial cells A6 (CCL102) were grown in 25-cm^2 flasks (Costar, Cambridge, MA) at room temperature (20–22 °C) with CL2-Amphibian medium (NIH-Media Section, Bethesda, MD), 2 mM glutamine, 10% fetal bovine serum, and 1% antibiotic-antimicotic solution, without gas control. Cells at confluence were harvested with 0.25% trypsin-1 mM EDTA (GIBCO-BRL), plated in very small numbers and transferred to a confocal imaging chamber, Model RC30 (Warner Instrument Corp.). For studying the cells in an inverted gravitational orientation (upside down), they were platted in one of the surfaces of a sealed double coverslip chamber that was turned upside down. Four A6 cells were observed for each gravitational orientation.

B. Video microscopy and lateral radial profiles of the cells

For microscopy imaging and time lapse recordings was used an inverted Zeiss Axiomatic phase-contrast microscope (25× objective magnification) equipped with a Dage-MTI video camera and a Metamorph image processing software (Universal Imaging). The plasma membrane fluctuations of individual cells were recorded at regular time intervals of 30 s, using the NIH-Image software [17]. Typical movies for lamellipodial dynamics in A6 cells cultured under normal and inverted gravitational orientation are supplied in Ref. [18]. The spatial resolution of the digitized images was such that 10 pixels correspond to 1 μm. For each movie frame, the high-resolution images of the plasma membranes were mapped into radial profiles containing the distances of all membrane pixels to the cell mass centers. These profiles were generated as follows. First, from the coordinates (x_i, y_i) of every membrane pixel i, $i=1,2,\ldots,N$, the cell center of mass

$$x_{cm} = \frac{1}{N}\sum_{i=1}^{N} x_i, \tag{1}$$

$$y_{cm} = \frac{1}{N}\sum_{i=1}^{N} y_i \tag{2}$$

is calculated. Typically, $N \sim 2\times 10^3$ data points have been used to build a radial profile. Second, the distance of every membrane pixel to this mass center $r_i = \sqrt{(x_i - x_{cm})^2 + (y_i - y_{cm})^2}$, and its azimuthal angle $\theta_i = \arctan(x_i/y_i)$ were determined. So, as shown in Fig. 1, the radial profile is given by the sequence of the distances r_i at the angle θ_i.

C. Data analysis

After obtaining the profiles as described in Sec. II B, it was possible to have an insight of the mechanism generating such signals by estimating the scaling exponent α in their power spectrum. The discrete Fourier transformation of the radial profile $r(\theta)$ given by

$$\tilde{r}(q) = \frac{1}{N}\sum_{k=0}^{N-1} r(\theta_k)\exp\left(\frac{2\pi i k q}{N}\right) \tag{3}$$

was calculated for each observation time. Here, N is the total number of cell contour pixels and $q=0,1,2,\ldots,N-1$ is the mode or frequency. The power spectrum is defined as $|\tilde{r}(q)|^2$ and the exponent α corresponds to the slope of the linear region in the FFT power spectrum of the profile after log transformation of frequency and power. This FFT regression is one of the better and computationally faster methods to

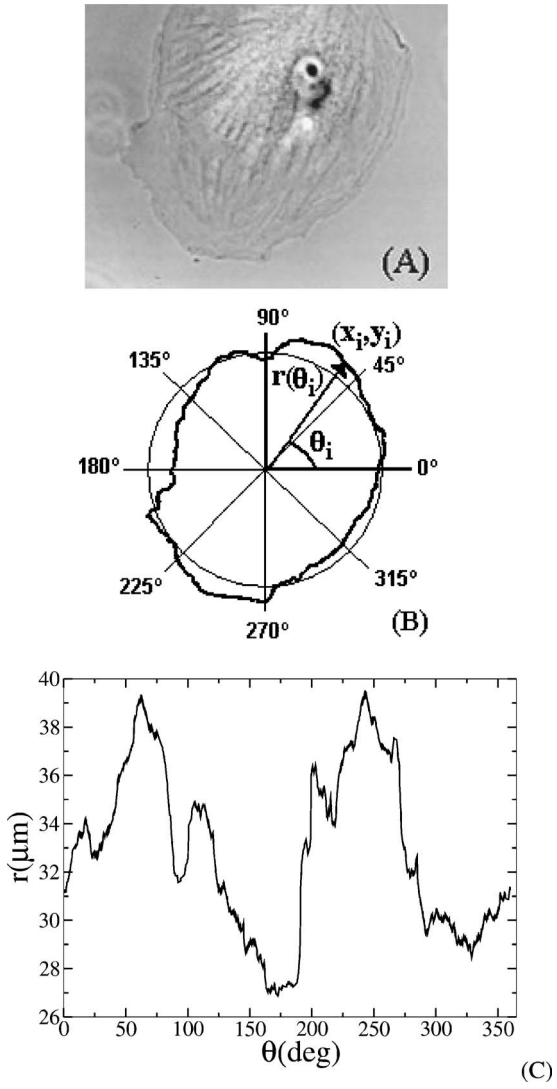

FIG. 1. (A) Typical A6 cell cultured at room temperature (about 20–22 °C) and (B) its digitized membrane contour. (C) Corresponding lateral radius profile, i.e., distances of the bordering membrane points to the cell mass center as a function of their angles measured as indicated in Fig. 1(b).

estimate the exponent α in $1/f^{\alpha}$ noise for large series ($N > 1000$) [19].

Also, the nature of the correlations in the radial profiles could be investigated through the analysis of the width W in the ϵ scale given by

$$W_N(\epsilon,t) = \frac{1}{N}\sum_{i=1}^{N} w_i(\epsilon,t), \tag{4}$$

with the local roughness $w_i(\epsilon,t)$ defined as

$$w_i(\epsilon,t) = \sqrt{\frac{1}{2\epsilon+1}\sum_{j=i-\epsilon}^{i+\epsilon}[r(\theta_j,t)-\bar{r}_i(t)]^2}, \tag{5}$$

where $\bar{r}_i(t)$ is the mean radius on the interval $[\theta_{i-\epsilon}, \theta_{i+\epsilon}]$ centered on the angle θ_i. For self-affine profiles, the width W scales as a power law [20],

$$W(\epsilon,t) \sim \epsilon^{H}. \tag{6}$$

The width W can distinguish two possible types of profiles. If the landscape is random, or even exhibits a finite correlation length extending up to a characteristic range (such as in Markov chains), $W \sim \epsilon^{1/2}$ as in a normal random walk. In contrast, if there is no characteristic length (infinitely long range correlations) then the width W scales as a power law

$$W(N) \sim \epsilon^{H}, \tag{7}$$

with the Hurst exponent $H \neq \frac{1}{2}$. $H > \frac{1}{2}$ implies that the profile presents persistent correlations, whereas $H < \frac{1}{2}$ means antipersistent correlations, i.e., sequences of increasing radii are more likely to alternate with others in which the radii decrease. For $1/f^{\alpha}$ data series the Hurst exponent H can be used to estimate the α exponent through the relationship $\alpha = 2H+1$ [19].

Finally, the temporal autocorrelation function

$$\phi_m(\theta_i) = \frac{1}{K}\sum_{j=1}^{K} r(\theta_i,t_j)r(\theta_i,t_j+m\Delta t) \tag{8}$$

for the radius at several fixed membrane points θ_i was evaluated. $\Delta t = 30$ s is the time lapse between successive frames. This function measures the similarity of the signal along time. For chaotic and stochastic signals $\phi_m \to 0$ as $m \to \infty$, whereas it is periodic in the case of periodic time series. Typically, $K \sim 300$ data points have been used to evaluate the temporal autocorrelation function.

III. RESULTS

Here, the experimental findings for ruffle oscillations bordering the plasma membrane in A6 amphibian cells cultured under normal and upside down conditions are presented.

A. Normally oriented cells

Figure 2 presents the power spectrum and the width W in the ϵ scale of a typical membrane edge profile. The slope of the linear regions in both log-log plots indicate that the instantaneous cell contours are long-range persistent correlated. At different observation times the values of the exponents α and H for this particular cell vary around the mean values $\alpha \sim 2.81$ and $H \sim 0.79$ (see Fig. 3). So, the spatial contours generated by membrane fluctuations in A6 cells are self-affine with a $1/f^{\alpha}$ power spectrum over at least two decades at low frequencies.

The temporal patterns of edge ruffle fluctuations were analyzed through the radius autocorrelation functions $\phi_m(\theta)$ for different membrane points θ. Figure 4 shows the two characteristic regimes observed for ϕ_m: an exponential decay [Fig. 4(a)] and a periodic oscillatory behavior [Fig. 4(b)]. From Fig. 4(a), a decay time $\tau \sim 36$ min is obtained for the normally oriented A6 cell of Fig. 1(a) at a fixed angle of 185°. However, the ruffle decay times exhibit a nonhomogeneous angular distribution along the plasma membrane. For the A6 cell in Fig. 1(a), there exist membrane sectors with higher ruffle activities (decay times of ~10 min) and others

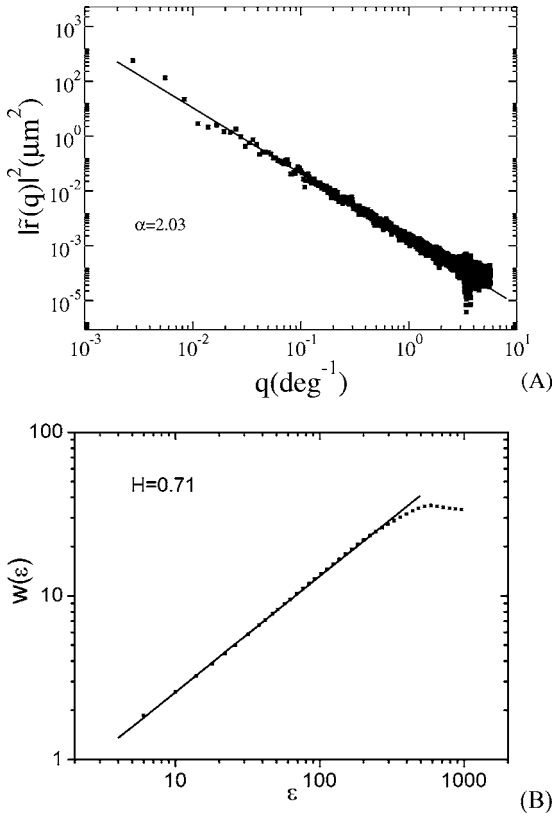

FIG. 2. Typical (A) power spectrum and (B) width or roughness in ϵ scale of membrane border profile at a given observation time. The linear portions in both power spectra and width curves indicate that membrane contours of A6 cells are rough and long-range correlated. The unit of ϵ corresponds to an arc of 0.36°.

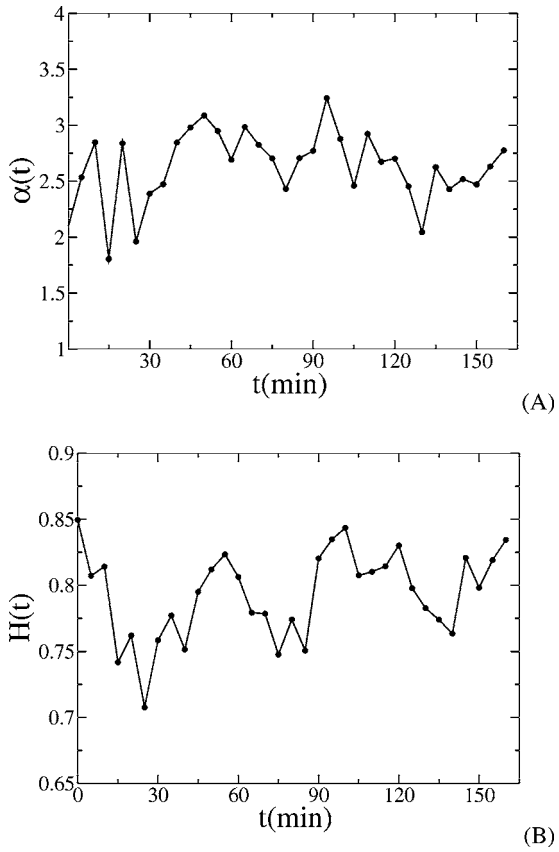

FIG. 3. Evolution in time of the exponents (A) α and (B) H measured for a typical normally oriented A6 cell.

with lower activities (decay times of ~40 min). In the highly active membrane regions, fast lamellipodial extension and retraction cycles used to explore the extracellular environment are observed.

The exponential decay of the temporal autocorrelation function ϕ_m, also observed for small random fluctuations of murine macrophages [15,16], is the dominant behavior except in a few membrane regions which display neat undamped oscillatory autocorrelations. In these regions, cycles of lamellipodia extension and receding typically occur at periods of about 45 min, as shown in Fig. 4(b). Such membrane sectors seem to correspond to cell attachments (focal contacts) to the surface of the culture plate. For comparison, defining the frequency of occurrence of ruffles as the number of structures formed at the same region of the membrane per minute, a value of 0.5 ruffles/min was measured for macrophages at 37 °C. This leads to a "period" (mean interval between successive ruffles) of 2 min that is roughly quadruplicated at a lower temperature of 24 °C [16]. Also, lamellipodia in primary chick embryo heart fibroblasts [21] and B16F1 mouse melanoma cells [22] form and move around on a time scale of minutes.

B. Cells upside down

As shown in Figs. 5(b), 5(c), and 6, the same qualitative results, i.e., self-affine spatial contours with a $1/f^{\alpha}$ power spectrum and random temporal membrane fluctuations except in certain cell attachment points, have been found for A6 cells cultured upside down. In the case of the cell used to obtain these figures, the mean values $\alpha \sim 2.96$ and $H \sim 0.72$ were obtained. Also, its temporal autocorrelation function reveals a neat quasiperiodic behavior close to the membrane regions from which the cell attaches to the surface of the culture plate [see Fig. 6(b)]. Finally, the sizes of the zones with longer ruffle decay times decrease and the distribution of those zones with slower ruffle dynamics becomes more uniform along the membrane, suggesting that its overall activity is enhanced.

Table I summarizes the results for the spatiotemporal characterization of the membrane ruffle fluctuations in A6 amphibian cells cultured under different gravitational orientations. For each A6 cell, the listed values of α and H are temporal averages over the correspondent values obtained at all observation times of that cell. A multivariate analysis based on the Hotelling T^2 test [23] was used in order to compare the vector of means $(\bar{\alpha}, \bar{H})$. The result showed significant difference at any level of significance equal or greater than 5.26% between these two groups of cultured cells. In addition, the Bonferroni simultaneous confidence intervals [23] revealed that there was a significant difference ($p < 0.05$) between the power spectrum exponents α, but not between the Hurst exponent H ($p > 0.05$), for normally oriented and upside down A6 cells. So, concerning the Hurst exponent H it can be said, with a 95% chance of being cor-

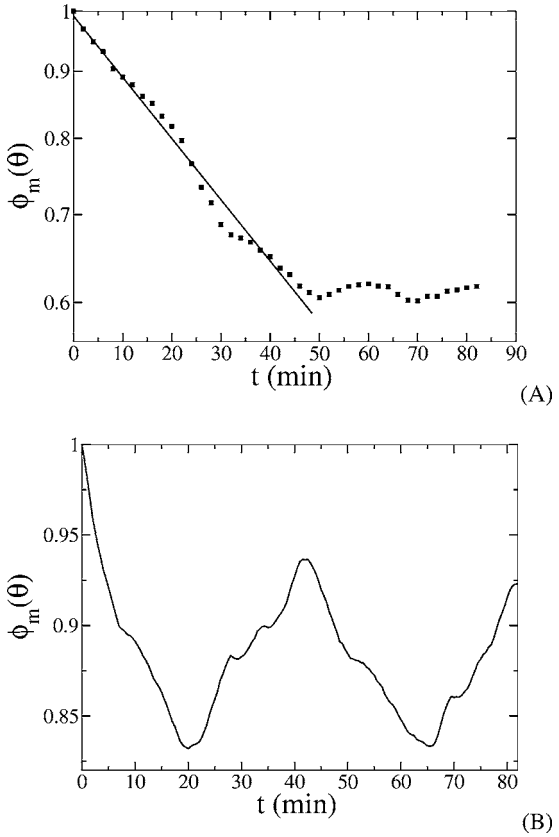

FIG. 4. (A) The temporal autocorrelation functions for the large majority of membrane points exhibit an exponential decay, but in very few regions (B) an oscillatory behavior is observed. The solid line in (A) corresponds to a nonlinear fitting $y=y_0+a_1\exp(-x/\tau)$, with $\tau=35.75$ min indicating a slow ruffle dynamics. The $\phi_m(\theta)$ values were normalized to the unity.

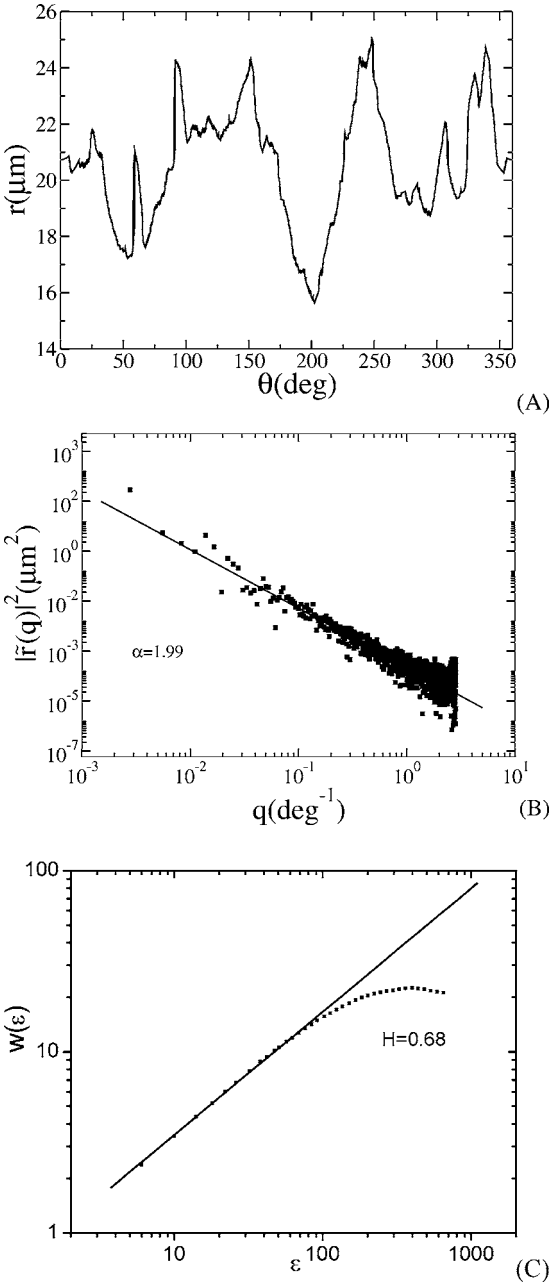

FIG. 5. (A) Typical membrane edge profile of an A6 cell cultured upside down at a given observation time. Corresponding (B) power spectrum and (C) width in ϵ scale of the radius profile in (A). Again, the linear portions in both power spectra and width curves indicate that the membrane contours of upside down A6 cells are rough and long-range correlated. The unit of ϵ corresponds to an arc of 0.36°.

rect, that the exponent mean value is the same for those two groups of A6 cells. In turn, for the α exponent, the hypothesis of equal means is rejected, indicating that the exponents are different. Taking into account a significance level of 5% and since the experience from research on surface growth shows that the Hurst exponent is, in general, more accurately estimated from experimental data than the power spectrum exponent, we decided in favor of the statistical equality between these two groups. Consequently, we are suggesting that different gravitational orientations had none or little effect on the shape of the borders of ruffling membranes.

A similar statistical analysis was performed for the decay times and periods of the temporal autocorrelation functions. Again, the different gravitational orientations had no significant effect, at the significance level of 5% on the measured values of the ruffle decay times. In contrast, the periods of the temporal autocorrelation functions nearby focal contacts in normally oriented A6 cells are significantly altered from those corresponding to upside down cultured cells. In practical terms, the present experiment demonstrates that in A6 cells the different gravitational orientations affect only the lamellipodium periodic oscillations nearby focal contacts.

IV. DISCUSSION

The results previously reported suggest the following picture for the dynamics of membrane ruffles in A6 cells. Except in some few discrete regions, their plasma membranes exhibit cycles of lamellipodia protrusion and receding leading to long-range, persistent correlated radius profiles along their border. Such edge ruffles appear and retract randomly in time, as confirmed by temporal autocorrelation functions

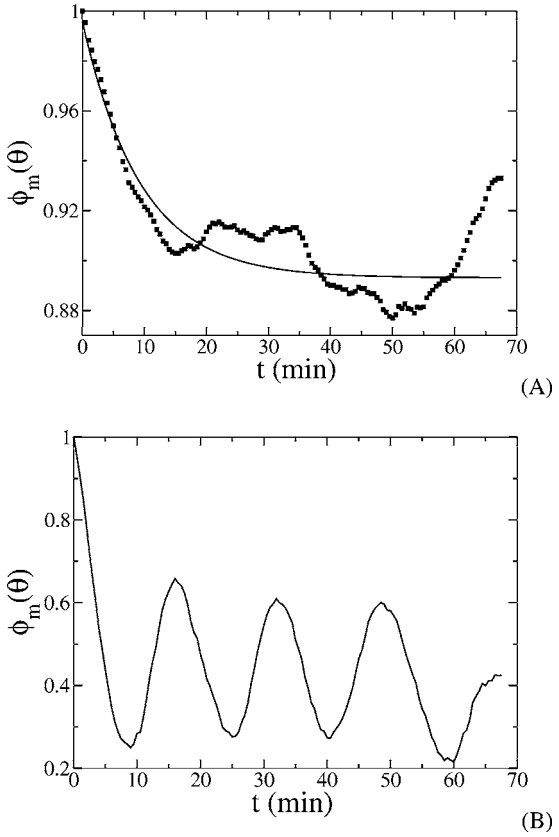

FIG. 6. For A6 cells cultured upside down, again the autocorrelation functions exhibit two distinct behaviors: (A) an exponential decay for the large majority of membrane points and (B) a quasiperiodic regime in very few regions. The solid line in (A) corresponds to a nonlinear fitting $y=y_0+a_1\exp(-x/\tau)$, with $\tau=9.36$ min indicating a fast ruffle dynamics. The $\phi_m(\theta)$ values were normalized to the unity.

decaying exponentially. The characteristic decay time of these dynamic structures in membrane regions with higher lamellipodium activity was estimated from the autocorrelation function as $\tau\sim 10$ min at 22 °C, well within the time scale of minutes observed for other cell types [15,16,21,22]. In turn, in membrane zones with low lamellipodium activity an average $\tau\sim 40$ min was found. This ruffling process is associated to the continual rearward motion of the lamellipodia observed in the repeated crawling movements of cells migrating through a fibroblast locomotion mode [1]. In turn, near the few discrete regions aforementioned, lamellipodia dynamics is roughly periodic and slower with a typical ruffling period of about 36 min, as illustrated by the temporal autocorrelation function shown in Fig. 4(b). These regions seem to be points of close adhesion to the substratum (focal adhesions) where integrins assemble to combine their weak affinities in order to reach enough adhesive capacity to promote cell anchorage.

A periodic (or quasiperiodic) oscillatory behavior of edge ruffles was not reported in Refs. [16,21]. In the case of macrophages, the reason is that they do not develop stress fibers or focal adhesions due to their rapid crawling [24]. Also, Felder and Elson [21] measured only ruffles in the leading, active edges of fibroblasts. To providing a working hypothesis, we suppose that active ruffling and lamellipodium formation are inhibited nearby focal adhesions, thereby explaining the lower frequency of edge ruffle formation neighboring focal adhesions. In agreement with Ref. [22], such inhibition could be triggered by a stabilized microtubular network, which is demanded for increase cell adhesion to the substratum. Indeed, at the front of migrating cells, the local integrin engagement in mature and persistent adhesions leads to Rac activation, which in turn induces recruitment and clustering of activated integrins and structural components, including microtubules that are stabilized by Rac. Then, a positive feedback is established, since microtubule polymerization activates Rac. In turn, at the rear of the cell, Rho activity leads to microtubules stabilization [25] and, again, to inhibition of edge ruffles. So, the question related to the periodicity of membrane border displacements in such adhesion points remains. Szabó *et al.* [9] measured periodic height fluctuations on the cell surface around stress fibers at the rear of quiescent 3T3 mouse fibroblasts. In contrast, they also found that membrane regions without apparent stress fibers nearby lack such sustained periodic fluctuations. Since focal adhesions are sites to which actin filaments are anchored and bundled together into stress fibers, we suggest in agreement with Ref. [9] that these periodic oscillations are induced by myosin driven contractions of stress fibers.

TABLE I. Exponents characterizing edge membrane fluctuations of A6 cells cultured in Petri dishes at the normal and upside down orientations.

Plate orientation	Cell specimen	Time averaged exponents			Dynamic parameters		
		power spectrum: α	Hurst: H	Mean values	period slow	decay time	Mean values
Normal	1	2.84±0.18	0.68±0.04		36±1	45±6	
	2	2.89±0.08	0.69±0.03	$\langle\alpha\rangle=2.86$	38±5	44±8	$\langle p\rangle=36.2$
	3	2.91±0.26	0.70±0.05	$\langle H\rangle=0.72$	27±4	38±5	$\langle\tau\rangle=39.5$
	4	2.81±0.16	0.795±0.001		44±7	31±7	
Upside down	1	2.77±0.16	0.82±0.04		19±3	45±7	
	2	2.53±0.25	0.58±0.05	$\langle\alpha\rangle=2.68$	17±6	40±8	$\langle p\rangle=19.7$
	3	2.60±0.27	0.68±0.07	$\langle H\rangle=0.70$	20±4	35±5	$\langle\tau\rangle=40.7$
	4	2.77±0.28	0.723±0.003		23±6	43±9	

The statistical analysis of the data in Table I indicates that the above picture for the dynamics of membrane ruffles is the same for normal and upside down cultured A6 cells. Indeed, different gravitational orientations had none or little effect on the structural parameters, such as power spectra and surface roughness, of these membrane ruffle fluctuations. Even some dynamic parameters, such as the decay time of ruffles, were not significantly altered. However, this is not true for the periods of lamellipodia oscillations near the focal adhesion points. Indeed, in A6 cells cultured upside down the periods of ruffle oscillations near adhesion points decrease to about one half of their typical values observed in normally oriented A6 cells. Since the only difference between these cultures is the orientation of the local gravitational field, such results are indicating that A6 cells react to gravity stimulus by slightly changing their cytoskeleton dynamics. So, the strength of focal adhesions, characteristic for cells cultured on flat and rigid substrates, is modulated by the cell. When cultured upside down, A6 cells reinforce their sites of mechanical anchorage to the surface plate in response to tensions enhanced by gravity. Functionally this is exactly what one would expect. Indeed, a necessary feature to make a large, mature focal adhesion is mechanical tension. Such reinforcement of focal adhesions due to the gravitational tension probably lead the cells to increase their signaling activity, as well as to an extensive rearrangement of the internally generated forces which are correlated with the state of aggregation of those focal adhesions [26,27].

Recent results from Döbereiner *et al.* [28] and Giannone *et al.* [29] for mouse embryonic fibroblasts (MEF) adhered on fibronectin-coated substrates reinforce our findings. These authors have established that the spreading of MEF cells proceeds through three phases of motility separated by two dynamic phase transitions neatly expressed in the active lamellipodia. Moreover, the contractile spreading phase is characterized by periodic local retractions of the lamellipodia that depends upon a stiff substrate, integrin binding, and myosin light chain kinase activation. The generation of periodic protrusion and contraction cycles in lamellipodia requires forces applied on rigid matrix-integrin-actin connections that trigger signals needed for focal adhesion formation, preferentially at the tips of the contracting lamellipodia. Hence the local, periodic oscillations observed in the present study of A6 cells seems to correspond to the periodic extension cycles of lamellipodia in MEF cells, which those authors hypothesize as being a general mechanism used by the cells to the mechanical probing of the extracellular matrix rigidity.

Future experiments are needed to determine the effects of an inverted gravitational orientation on cell motility and clustering organization, central in various situations such as embryo development, invasion and metastasis. In particular, essays are being designed to study the long term behavior of cells grown upside down. It is possible that the flicker fluctuations dynamics of the cell membranes at the steady state may differ from the results of the present work. Also, quantitative essays on cell motion (diffusion properties and velocity distribution functions), as recently done for Hydra [30] and glioblastoma cells [31], and cell-cell aggregation (cluster size distribution functions) of normal and tumor cells [32], are currently being designed. The use of new dissection microscopes able to discriminate different cell populations, e.g., invasive and metastatic cells, certainly will help to better understand the dynamics of cancer progression. In addition to the proposed experiments, immunocytochemical and immunobloting observations can be useful to study protein expression at cell membranes of cells under gravitational stress.

V. CONCLUSIONS

We have presented videomicroscopy results for the edge membrane fluctuations in amphibian A6 cells cultured under normal and inverted gravitational orientation. Such active oscillations were quantitatively characterized through the power spectrum and Hurst exponent of their spatial radial profiles, as well as their radius autocorrelation function in time. The results suggest that these edge ruffle fluctuations exhibit a stochastic dynamics with $1/f^{\alpha}$ power spectrum over at last two decades at low frequencies and long range correlated, self-affine lateral border profiles. Furthermore, the different gravitational orientations had none or little effect on the structure (power spectra and surface roughness) of these membrane ruffle fluctuations. Also, the decay times of ruffles remained statistically unchanged. However, the periods of lamellipodia oscillations near the focal adhesion points were significantly altered in A6 cells cultured upside down which seem to developed reinforced focal adhesions. It could be expected that these and future results concerning cell motility and collective organization under distinct mechanical inputs, particularly in different gravitational conditions, may provide useful tools for medicine and tissue engineering.

ACKNOWLEDGMENTS

The authors thank A. J. Regazi for performing the statistical analysis. M.J.V. and R.J. would like to acknowledge the hospitality at the NIH. This work is supported in part by the NIDCD Intramural Program and the Brazilian Agencies FAPEMIG and CNPq.

[1] D. Bray, *Cell Movements: From Molecules to Motility*, 2nd ed. (Garland Publishing, New York, 2001).

[2] F. Brochard and J. F. Lennon, J. Phys. (France) **36**, 1035 (1975).

[3] M. Chicurel, Science **295**, 606 (2002).

[4] P. Girard, J. Prost, and P. Bassereau, Phys. Rev. Lett. **94**, 088102 (2005).

[5] E. Sackmann, in *Handbook of Biological Physics Vol. 1A: Structure and Dynamics of Membranes. From Cells to Vesicles*, edited by R. Lipowsky and E. Sackmann (Elsevier

Science B. V., Amsterdam, 1995).
[6] S. Levin and R. Korenstein, Biophys. J. **60**, 733 (1991).
[7] N. S. Gov and S. A. Safran, Biophys. J. **88**, 1859 (2005).
[8] W. Häckl, M. Bärmann, and E. Sackmann, Phys. Rev. Lett. **80**, 1786 (1998).
[9] B. Szabo, D. Selmeczi, Z. Kornyei, E. Madarasz, and N. Rozlosnik, Phys. Rev. E **65**, 041910 (2002).
[10] B. Fabry, G. N. Maksym, J. P. Butler, M. Glogauer, D. Navajas, and J. J. Fredberg, Phys. Rev. Lett. **87**, 148102 (2001).
[11] K. Kruse, J. F. Joanny, F. Jülicher, J. Prost, and K. Sekimoto, Eur. Phys. J. E **16**, 5 (2005).
[12] R. A. Simha and S. Ramaswamy, Phys. Rev. Lett. **89**, 058101 (2002).
[13] K. Kruse, J. F. Joanny, F. Jülicher, J. Prost, and K. Sekimoto, Phys. Rev. Lett. **92**, 078101 (2004).
[14] U. Agero, L. G. Mesquita, B. R. A. Neves, R. T. Gazzinelli, and O. N. Mesquita, Microsc. Res. Tech. **65**, 159 (2004).
[15] U. Agero, C. H. Monken, C. Ropert, R. T. Gazzinelli, and O. N. Mesquita, Phys. Rev. E **67**, 051904 (2003).
[16] J. C. Neto, U. Agero, D. C. P. Oliveira, R. T. Gazzinelli, and O. N. Mesquita, Exp. Cell Res. **303**, 207 (2005).
[17] W. Rasband NIH image, 1.60, 1996, Washington, DC, http://rsb.info.nih.gov/nih-image/
[18] See EPAPS Document No E-PLEEE8-74-121609 to watch the movies of typical protrusion and contraction cycles in lamellipodia occurring in A6 cells cultured under normal and inverted gravitational orientations. For more information on EPAPS, see http://www.aip.org/pubservs/epaps.html
[19] P. Meakin, *Fractals, Scaling and Growth Far From Equilibrium* (Cambridge University Press, Cambridge, England, 1998).
[20] A. L. Barabási and H. E. Stanley, *Fractal Concepts in Surface Growth* (Cambridge University Press, Cambridge, England, 1995).
[21] S. Felder and E. L. Elson, J. Cell Biol. **111**, 2513 (1990).
[22] C. Ballestrem, B. Wehrle-Haller, B. Hinz, and B. A. Imhof, Mol. Biol. Cell **11**, 2999 (2000).
[23] R. A. Johnson and D. W. Wichern, *Applied Multivariate Statistical Analysis*, 4th ed. (Prentice-Hall, Englewood Cliffs, NJ, 1998).
[24] R. G. Painter, J. Whisenand, and A. T. McIntosh, J. Cell Biol. **91**, 373 (1981).
[25] A. Ridley, M. A. Schwartz, K. Burridge, R. A. Firtel, M. H. Ginsberg, G. Borisay, J. T. Parsons, and A. R. Horwitz, Science **302**, 1704 (2003).
[26] D. Choquet, D. F. Felsenfeld, and M. P. Sheetz, Cell **88**, 39 (1997).
[27] N. Q. Balaban, U. S. Schwarz, D. Riveline, P. Goichberg, G. Tzur, I. Sabanay, D. Mahalu, S. Safran, A. Bershadsky, L. Addadi, and B. Geiger, Nat. Cell Biol. **3**, 466 (2001).
[28] H. G. Döbereiner, B. Dubin-Thaler, G. Giannone, H. S. Xenias, and M. P. Sheetz, Phys. Rev. Lett. **93**, 108105 (2004).
[29] G. Giannone, B. J. Dubin-Thaler, H. G. Döbereiner, N. Kieffer, A. R. Bresnick, and M. P. Sheetz, Cell **116**, 431 (2004).
[30] A. Upadhyaya, J. P. Rieu, J. A. Glazier, and Y. Sawada, Physica A **293**, 549 (2001).
[31] A. Czirok, K. Schlett, E. Madarász, and T. Vicsek, Phys. Rev. Lett. **81**, 3038 (1998).
[32] R. L. Mendes, A. A. Santos, M. L. Martins, and M. J. Vilela, Physica A **298**, 471 (2001).